JPET Fast Forward. Published on March 2, 2005 as DOI: 10.1124/jpet.104.082990

JPET #82990

Identification of subunit-specific and antagonist-specific amino acid residues in the NMDA receptor glutamate binding pocket

Leo Kinarsky[1], Bihua Feng[1], Donald A. Skifter, Richard M. Morley, Simon Sherman, David E. Jane, and Daniel Monaghan. [1]The Eppley Research Institute (L.K., S.S.) and the Department of Pharmacology (B.F., D.A.S., D.T.M.) University of Nebraska Medical Center; and Department of Pharmacology, University of Bristol, Bristol, U.K. (R.M.M., D.E.J.).

Running title:

NR2 glutamate binding site models

Correspondence:

Daniel T. Monaghan, Ph.D.

Department of Pharmacology

985800 Nebraska Medical Center

Omaha, NE 68198-5800

402-559-7196, FAX: 402-559-7495,

e-mail: dtmonagh@unmc.edu

Pages: 19

Tables: 0

Figures: 6

References: 40

Number of words

Abstract: 243

Introduction: 607

Discussion: 1369

Abbreviations: CGS-19755, (2*R**,4*S**)-4-phosphonomethyl-2-piperidine carboxylic acid; EAB515; α-amino-5-(phosphonomethyl)[1,1'-biphenyl]-3-propanoic acid; LAOBP, leucine/arginine/ornithine binding protein; L-701,324, 7-chloro-4-hydroxy-3-(3-phenoxy)phenyl-2H-quinolinone; LY233536, (±)-6-(1H-tetrazol-5-ylmethyl)decahydroixoquinoline-3-carboxylic acid; LY339434, (2*S*,4*R*,6*E*)-2-amino-4-carboxy-7-(2-naphthyl)hept-6-enoate; PBPD, (2*R**,3*S**)-1-(biphenyl-4-carbonyl)piperazine-2,3-dicarboxylic acid; PEAQX, (R)-[(S)-1-(4-bromo-phenyl)-ethylamino]-(2,3-dioxo-1,2,3,4-tetrahydroquinoxalin-5-yl)-methyl]-phosphonic acid; PPDA, (2*R**,3*S**)-1-(phenanthren-2-carbonyl)piperazine-2,3-dicarboxylic acid; PPPA, (2*R**,4*S**)-4-(3-phosphonopropyl)piperidine-2-carboxylic acid; QBP, glutamine binding protein; *(R)*-AP5, *(R)*-2-amino-5-phosphonopentanoate; *(R)*-CPP, (*R*)-3-((2-carboxypiperazin-4-yl)propyl-1-phosphonic acid; *(R)*-CPPene, ((*R*,*E*)-4-(3-phosphonoprop-2-enyl)piperazine-2-carboxylic acid.

Section: Neuropharmacology

Abstract

The resolved X-ray crystal structures of the glutamate binding domain (S1/S2 domains) of the GluR2 and NR1 glutamate receptor subunits were used to model the homologous regions of the N-methyl-D-aspartate (NMDA) receptor's NR2 subunits. To test the predictive value of these models, all four stereoisomers of the antagonist 1-(phenanthren-2-carbonyl) piperazine-2,3-dicarboxylic acid (PPDA) were docked into the NR2B glutamate-binding site model. This analysis suggested an affinity order for the PPDA isomers of D-*cis* > L-*cis* > L-*trans* = D-*trans* and predicted that the 2-position carboxylate group of the *cis*-PPDA isomers, but not of the *trans*-PPDA isomers, may be interacting with histidine 486 in NR2B. Consistent with these predictions, *cis*-PPDA displays an 35-fold higher affinity for NR2B-containing NMDA receptors than *trans*-PPDA. In addition, mutating NR2B's H486 to phenylalanine decreased *cis*-PPDA affinity 8-fold, but had no effect on *trans*-PPDA affinity. In contrast, the NR2B H486F mutation increased the affinity of the typical antagonists (2*R**,4*S**)-4-phosphonomethyl-2-piperidine carboxylic acid (CGS-19755) and 4-(3-phosphonopropyl) piperidine-2-carboxylic acid (PPPA). In the NR1-based NR2 models, there were only 4 subunit-specific amino acid residues exposed to the ligand-binding pocket (and 6 in the GluR2-based models). These residues are located at the edge of the binding pocket, suggesting that large antagonists may be necessary for subtype-specificity. Of these residues, mutational analysis and modeling suggest that A414, R712 and G713 (NR2B numbering) may be especially useful for developing NR2C and NR2D-selective NMDA receptor antagonists, and that residues A414 and T428 may determine subunit variations in agonist affinity.

Introduction

(*S*)-Glutamate is the primary excitatory neurotransmitter in the vertebrate CNS. The fast, excitatory actions of (*S*)-glutamate are mediated by three types of glutamate-gated ion channel receptors, the *N*-methyl-D-aspartate (NMDA), kainate, and AMPA receptors (Watkins and Evans, 1981; Monaghan et al., 1989; Watkins et al., 1990). NMDA receptors have been extensively studied because of their roles in synaptic plasticity (Collingridge and Bliss, 1995), developmental plasticity (Bear et al., 1990), and neuropathology (Choi, 1992). Functional NMDA receptors are a heteromeric complex composed of NR1 subunits (NR1a-NR1h, representing eight alternative splice forms from one gene (Sugihara et al., 1992) and NR2 subunits (NR2A-NR2D, from four distinct genes; Ikeda et al., 1992; Monyer et al., 1992; Ishii et al., 1993; Monyer et al., 1994). Current evidence supports a tetrameric structure involving two NR1 subunits and two NR2 subunits (Laube et al., 1998). In addition, a nonessential NR3 subunit has been identified (Sucher et al., 1995).

The glutamate binding sites of the NMDA receptor complex are found on the NR2 subunits (Laube et al., 1997; Anson et al., 1998). While the different NR2 subunits display generally similar pharmacological profiles (Ikeda et al., 1992; Buller et al., 1994; Laurie and Seeburg, 1994) some glutamate site agonists and antagonists can distinguish between the different NR2-containing receptors (Buller et al., 1994; Buller and Monaghan, 1997; Auberson et al., 2002; Feng et al., 2004). Accordingly, glutamate site agents can distinguish four different native NMDA receptors in brain that correspond both anatomically and pharmacologically to the four different NR2 subunits (Monaghan et al., 1988; Beaton et al., 1992; Christie et al., 2000). Since the different NR2 subunits

are heterogenously distributed, (Monyer et al., 1992; Watanabe et al., 1993; Buller et al., 1994) and display significantly different physiological properties (Monyer et al., 1994), antagonists that selectively block different NR2-containing NMDA receptors are likely to have markedly different physiological and therapeutic/adverse effects. To date, however, only a few glutamate-site antagonists have been found to display subtype selectivity and these compounds are only weakly selective. To facilitate the development of antagonists with greater subtype selectivity, we generated molecular models of the glutamate binding site on rat and human NR2 subunits.

The glutamate binding site on the glutamate-gated ion channel receptors lies in two domains, S1 and S2, which together have homology to the distantly-related bi-lobed bacterial amino acid binding proteins LAOBP (leucine/arginine/ornithine binding protein) and QBP (glutamine binding protein) (Nakanishi et al., 1990; O'Hara et al., 1993). Previously, Laube and colleagues have used the resolved structure of LAOBP (Oh et al., 1993) to generate a model of the NR2B subunit's glutamate binding site (Laube et al., 1997). This model, together with the use of site-directed mutagenesis, enabled the identification of amino acid residues that are critical for the binding of glutamate and glutamate-site antagonists. More recently, the AMPA receptor GluR2 subunit (Armstrong et al., 1998; Armstrong and Gouaux, 2000) and the NMDA NR1 (Furukawa and Gouaux, 2003) subunit S1/S2 domain structures have been resolved by crystallography. Since the NR2 subunit primary structure is more closely related to NR1 and GluR2 than to LAOBP, we used the resolved NR1 and GluR2 crystal structures to generate homology models of the NR2 S1/S2 structures. In support of this approach is the observation that the secondary structures of LAOBP/QBP and the distantly related

GluR2 are readily superimposed despite low sequence identity (Armstrong et al., 1998). To test the predictive value of the models, we evaluated mutations that were predicted to have specific effects on antagonist binding. We also tested point mutations of amino acid residues that were predicted to be subunit-specific to determine if these residues can account for some observations of pharmacological subunit-specificity.

Materials and Methods

Homology modeling. NR2B sequences D403 to N542 (S1) and K669 to N803 (S2) and the corresponding NR2C sequence were aligned to the GluR2 sequence. The COMPOSER and BIOPOLYMER modules of the SYBYL 6.6 (Tripos Inc., St. Louis) software package were used for comparative molecular modeling of the NR2B and NR2C subunits based on the crystal structure determined for GluR2(Armstrong et al., 1998).

Consistent with the GluR2 data, a disulfide bridge was formed between NR2B C746 and C801. Within the NR2 sequences there is a segment of 35 amino acids that has no homology to GluR2 (amino acids 422-456 of NR2B) and 21 amino acids of this NR2B segment are an additional insert relative to the GluR2 sequence. To model this loop, the loop searching method implemented in the SYBYL 6.6 was used to find the most appropriate protein loop from the Protein Data Bank (PDB). From the several candidates, the best fitting loop was chosen based on the high homology with the modeled sequence, the proper positioning of the anchor atoms, and the tight packing with the rest of the molecule. The constructed structural models were tested with the PROTABLE module and refined by energy minimizations using the AMBER (Kollman all-atom) force field implemented in SYBYL. To better model antagonist interactions with the NR2 subunits, the NR2B model was refit to the antagonist-bound conformation of the GluR2 subunit (Armstrong and Gouaux, 2000). Using these same methods, the recently resolved NR1 S1/S2 crystal structure in the antagonist-bound conformation was used to model each of the four human NR2 S1/S2 domains. Antagonist isomers were constructed in the ionized forms and energy-minimized using MMFF94 force field in SYBYL. Docking was performed with the DOCK software module of SYBYL 6.6.

Construction of rat NR2B point mutations. NR1a cDNA in pBluescript was generously provided by Dr. Shigetada Nakanishi and the NR2B cDNA in pRK5 was kindly provided by Drs. Dolan Pritchett and David Lynch. NR2B A414R, NR2B G427E, NR2B T428G, NR2B G712S, NR2B R712P/G713R, and NR2B H486F mutations were made using the QuikChange Site-Directed Mutagenesis Kit (Stratagene, La Jolla, CA). Mutations were confirmed by sequencing on both strands by the Molecular Biology Core Laboratory at the University of Nebraska Medical Center.

In Vitro transcription and translation in Xenopus oocytes. Plasmids were linearized with *Not*I (NR1a) or *Sal*I(NR2B) and transcribed with T7 (NR1a) or SP6 (NR2B) *in vitro* using the mMessage mMachine kit (Ambion, Austin, TX). Xenopus laevis female frogs were obtained from Xenopus I (Dexter, MI) and oocytes were isolated and prepared as previously described (Monaghan and Larson, 1997). The handling of frogs was performed in accordance with the Guide for the Care and Use of Laboratory Animals as adopted and promulgated by the U.S. National Institutes of Health. Oocytes were injected with 2-30 ng NR1/NR2 RNA (1:3) in 9 - 50 nL and then incubated in ND-96 (96 mM NaCl, 2 mM KCl, 1.8mM $CaCl_2$, 1mM $MgCl_2$, 5mM HEPES, pH 7.6) at 17°C for 1-4 days.

Oocyte electrophysiology. Electrophysiological responses of recombinant receptors expressed in Xenopus oocytes were measured by two-electrode voltage clamp (OC-725B Oocyte Clamp, Warner Instruments, Hamden, CT) at a holding potential of -60mV. Unless indicated otherwise, NMDA receptor responses were evoked by bath application of 10 μM (S)-glutamate / 10 μM glycine. Recordings were made in barium Ringer's solution to eliminate calcium-activated chloride currents. Only cells which generated

stable plateau responses were used. Current responses to drug application were recorded on both a strip-chart and by digital capture using an ITC-16 computer interface (Instrutech, Great Neck, NY) and a MacIntosh computer with AxoData software (Axon Instruments, Foster City, CA). Dose-response curves for antagonist blockade of responses were fit (GraphPad Prism, ISI Software, San Diego, CA) to the equation: $I = Imax/[1+(IC_{50}/A)]$, where I is the current response, Imax is the current response in the absence of antagonist, and A is the concentration of antagonist. (S)-Glutamate affinities were obtained for wild type and mutant receptors with the same set of solutions and used to correct antagonist IC_{50} values to the corresponding Ki values.

Materials: Antagonists were kindly provided by Dr. Paul Ornstein (PPPA) and Dr. Richard Lovell (CGS-19755). *Cis*-PPDA, *trans*-PPDA and (*R*)-CPPene were synthesized in our laboratory (Dr. Jane's). Other chemicals were obtained from Sigma Chemical (St. Louis, MO).

JPET Fast Forward. Published on March 2, 2005 as DOI: 10.1124/jpet.104.082990
This article has not been copyedited and formatted. The final version may differ from this version.

Results:

The rat NR2B and NR2C structural models were built by homology modeling based upon the GluR2 crystal structure (Armstrong et al., 1998; Armstrong and Gouaux, 2000). These are shown in Figure 1A superimposed upon the GluR2 crystal structure. The four human NR2A – NR2D S1/S2 models were constructed using the resolved NR1 subunit structure (Furukawa and Gouaux, 2003); the human NR2B S1/S2 structural model is shown in Figure 1F. The models underwent several rounds of energy minimizations with subsequent stereochemistry testing by the PROTABLE module of SYBYL. From 275 amino acid residues included in each of the models, four to nine residues, mostly from the less defined loop 422-456, had backbone conformations that fell into disallowed areas of the Ramachandran plot; while 12-19 residues were found within allowed, but sterically-constrained areas of the Ramachandran plot. Given the high degree of overall structural similarity between the resolved crystal structures for GluR2 and the distantly related LAOBP and QBP, the proposed structure for NR2s (which are much more closely-related to GluR2 and NR1) may have predictive value. Recently, a model for the human NR2B subunit based upon the GluR2 subunit was generated (Tikhonova et al., 2002), it is not known, however, how this model compares to the NR2B models described here.

<u>Docking of PPDA to NR2B</u>:

In recent studies, we have identified the compound *cis*-PPDA as a high affinity NMDA receptor antagonist with novel subtype selectivity (Feng et al., 2004). For the structure of PPDA and other antagonists used and discussed in this study, see Figure 2. As a test of the predictive value of the models generated, we modeled the binding of

PPDA to NMDA receptors because PPDA has a bulky phenanthrene group attached to dicarboxypiperazine via a carbonyl group. Thus, this large and relatively rigid compound is expected to have relatively few permitted modes of docking with the NR2 glutamate binding site. Furthermore, PPDA docking was of interest because PPDA is unusual for an NMDA receptor antagonist in having two closely-spaced acid groups (3.4 Å) which do not conform to the previously defined NMDA receptor antagonist pharmacophore (6 - 7 Å between acid groups; Ortwine et al., 1992; Whitten et al., 1992). The energy-minimized (MMFF94 force field) (2*S*,3*S*)-, (2*S*,3*R*)-, (2*R*,3*R*)- and (2*R*,3*S*)-isomers of PPDA were constructed. For each of these isomers, four initial conformations were used which differed in piperizine ring conformation (chair or boat) and in the position of the phenanthrene ring relative to the dicarboxylic acids ("cis" or "trans"). After energy minimization, each isomer of PPDA was manually docked into the NR2 glutamate binding site using the DOCK module of SYBYL. To dock PPDA, the 4-amino and 3-carboxy groups of PPDA (corresponding to the α-amino and carboxylate groups of glutamate, respectively) were superimposed upon corresponding positions determine for the kainate molecule within the GluR2 crystal structure (while GluR2 was superimposed onto NR2B). After docking, the PPDA-receptor complex was energy-minimized to improve the fit. The three bonds in PPDA that can rotate were allowed to rotate, as were the ligand-binding amino acid residue side chains (see Figure 1 D). In docking the different isomers of PPDA, and performing several rounds of energy minimizations for each isomer, we found that the two *cis* isomers ((2*R*,3*S*)- and (2*S*,3*R*)- isomers) displayed lower energy fits (-231 kcal and –274 kcal, respectively) than any of the *trans* isomers (-167 kcal for (2*S*,3*S*) isomer and –159 kcal for the (2*R*,3*R*) isomer). In Figure 1B, the

(2*R*,3*S*)-isomer (L-*cis*) of PPDA is shown docked. Interestingly, for all isomers/conformations, the large and rigid phenanthrene ring group was consistently fit into, or near, a groove at the bottom of the S1/S2 cleft formed between helix F and helix H on the S2 interface (Armstrong et al., 1998). This places the phenanthrene ring pointing directly out of the binding cleft and perpendicular to the two beta strands that link the S1/S2 lobes.

The proposed placement of the phenanthrene group is identical to the position of the bulky aliphatic group of kainate (and presumably domoate) when bound to GluR2 (Armstrong et al., 1998). This orientation for a large hydrophobic group is also consistent with that proposed for the biphenyl group of the NMDA receptor antagonist EAB-515 (α-amino-5-(phosphonomethyl)[1,1'-biphenyl]-3-propanoic acid) (Bigge, 1993). In antagonist molecular modeling studies, it was proposed that the linear biphenyl group of EAB-515 is nearly perpendicular to the plane formed by the α-amino and the two carboxy groups of EAB-515 and occupies a "hydrophobic pocket" (see also Cheung et al., 1996). Thus, the proposed hydrophobic pocket, is probably the interface between the S1 and S2 lobes and our model predicts that it might include the groove formed between helix F and helix H. In this docking, the end of the phenanthrene ring is flush with the surface of the S1/S2 globular structure and is in the vicinity of the subunit-specific residues NR2B R712 and G713.

Subsequent to docking the PPDA isomers, we were able to synthesize the racemic *trans* isomer of PPDA and compare it to the racemic *cis* isomer at recombinant NMDA receptors. The *cis* and *trans* forms of PPDA were tested at various concentrations for their ability to inhibit NR1a/NR2B NMDA receptor responses evoked by 10μM

glutamate and 10μM glycine. Agonists were applied until a steady response was obtained and then increasing concentrations of antagonist were applied, followed by an agonist-only application (for an example see figure 3 of Feng et al., 2004). As predicted, the *cis* isomer displayed a significantly higher affinity (Figure 3B, Figure 4B). NR1a/NR2B affinity for *cis*-PPDA was 0.26 ± 0.05 μM and for *trans*-PPDA, 9.1 ± 1 μM. The NR2B wild type 100% response was 81 ± 13 nA (mean ± s.e.m.); the NR2B H486F 100% response of 68 ± 13 nA.

As mentioned above, PPDA is distinctive among NMDA receptor antagonists in having the two closely spaced acidic groups which are separated by only three carbon-carbon bonds. Most NMDA receptor antagonists have two acidic groups separated by 5 or 7 carbon-carbon bond lengths. The PPDA docking shown in Fig. 1B suggests that the closely spaced acidic groups in *cis*-PPDA may place the 2-carboxy group of *cis*-PPDA in a position to interact with NR2B H486. In contrast, lowest energy fits for *trans*-PPDA point the 2-carboxy group away from NR2B H486. Experiments using site-directed mutagenesis suggest that this residue has no effect on *(R)*-AP5 (*(R)*-2-amino-5-phosphonopentanoate) or *(R)*-CPP binding (Laube et al., 1997). Thus, our model of *cis*-PPDA docking predicts that H486 may have a specific interaction with *cis* –PPDA that is not shared with the typical competitive antagonists. Furthermore, modeling predicts that *trans*-PPDA and *cis*-PPDA would be differentially affected by mutating H486.

To test these predictions, we constructed the NR2B H486F mutation and evaluated the potency of *cis*- and *trans*-PPDA and the antagonists CGS-19755 and , (2*R**,4*S**)-4-(3-phosphonopropyl)piperidine-2-carboxylic acid (PPPA). The latter two antagonists are partially constrained in an extended form by a piperidine ring and display 5 and 7 carbon-

carbon bonds between their acid groups, respectively. Changing the histidine to phenylalanine resulted in functional NMDA receptors with a 6-fold reduced affinity for (*S*)-glutamate (wt: 2.3 ± 0.2 μM; H486F: 13.5 ± 0.7 μM). This compares well with the results of (Laube et al., 1997; Anson et al., 1998) which reported an 8 – 10 fold reduction in glutamate affinity with this mutation. Whereas the antagonists CGS-19755 and PPPA displayed a 2- to 3-fold increase in receptor affinity for NR1/NR2B-H486F (Figures 3, 4), *cis*-PPDA displayed more than a 8-fold reduction in affinity (wt: 0.26 ± 0.05 μM; H486F: 2.2 ± 0.3 μM). Also, as predicted by the modeling, *trans*-PPDA was not affected by the H486F mutation (wt: 9.1 ± 1.0 μM; H486F: 8.4 ± 0.6 μM).

Subunit-specific amino acids in the NR2 Glutamate Binding Pocket.

Evaluation of the NR2 models based on GluR2 indicated that the ligand-binding pocket is highly conserved between different subunits. As shown in figure 1C, there are a large number of amino acids that vary among at least one of the NR2 subunits (magenta-shaded residues). However, only eight residues of the 39 residues lining the ligand-binding pocket are not identical among all 4 NR2 subunits. All of these residues are at the edge of the ligand-binding pocket and are not likely to directly interact with *(S)*-glutamate or similarly-sized antagonists. Of these residues, the two flanking NR2B I490 have side chains that are not directed toward the pocket. The NR1-based homology models predicted the same subunit-specific residues in the ligand-binding pocket as the models based on GluR2, except for NR2B residues G427 and T428. These two residues are on the loop that is not present in GluR2 but is partially present in NR1. The NR1-based modeling procedure placed this loop outside of the ligand-binding cleft region (Figure 1F). The remaining subunit-specific amino acid residues in the ligand-binding

pocket were: (NR2B numbering) A414 which corresponds to an arginine on NR2C, R712 – corresponding to a proline on NR2D, G713 which corresponds to a serine on NR2C and an arginine on NR2D (Figures 1D, 1E, and 4). The amino acids lining the binding pocket are also well conserved between human and rat; R711 of rat NR2A is the only ligand-binding pocket residue to differ in the human sequence (lysine).

Pharmacological effects of select point mutations.

Our results suggest that most antagonists and agonists generated to date are unlikely to interact with the proposed subunit-specific residues. Nevertheless, we sought to determine if any of these residues could explain some of the subunit specificity observed to date.

A414R: The homology models generated suggest that NR2B's A414 is near the glutamate binding pocket (Figure 1D, 1E) and is replaced by an arginine in NR2C and NR2D (Figure 5). Both NMDA and (*S*)-glutamate display higher affinity at NR2C and NR2D than at NR2B. Converting NR2B's alanine to arginine, as found in NR2C and NR2D, significantly increased the affinity of both of these agonists (Figure 6A). (*S*)-Glutamate: (wt: 2.3 ± 0.2 μM; A414R: 0.95 ± 0.10 μM), NMDA: (wt: 29.9 ± 0.2μM; A414R: 9.7 ± 0.4μM). However, the potency of the antagonist LY233536 ((±)-6-(1H-tetrazol-5-ylmethyl) decahydroixoquinoline-3- carboxylic acid), which has lower affinity at NR2C and NR2D than at NR2B (Buller and Monaghan, 1997), was not affected by the A414R mutation (wt: 0.56 ± 0.01μM; A414R: 0.50 ± 0.01μM). The average 100% response of the NR1a/NR2B A414R receptor was 51 ± 4 nA (mean ± s.e.m.). The average 100% response of the NR1a/NR2B receptor observed with this and the below mutation studies was 73± 11 nA.

G427E The residue adjacent to NR2B's 428 is also subunit-specific with the NR2A subunit displaying a glutamate residue while the other NR2 subunits each have glycine at this position. The antagonist LY233536 is distinctive in having a several fold higher affinity for receptors containing NR2B subunits than for NR2A subunits (Buller and Monaghan, 1997). G427 does not appear to contribute significantly to LY233536 selectivity since the mutating G427 to glutamate caused only a small change in LY233536 affinity (wt: 0.56 ± 0.01μM; G427E: 0.78 ± 0.02μM), nor did it greatly affect agonist affinity (NMDA: wt: 29.9 ± 0.2μM; G427E: 37.8 ± 2.3μM; (*S*)-glutamate: wt: 2.3 ± 0.2μM; G427E: 2.9 ± 0.2μM) (Figure 6B). The average 100% response of the NR1a/NR2B G427E receptor was 63 ± 7 nA.

T428G: In NR2C, NR2B's T428 is replaced by glycine. In the GluR2-based models, these residues are at the edge of the S1/S2 cleft (Figure 1D). To test if T428 might contribute to agonist or antagonist binding, we constructed the NR2B T428G mutation. In addition to testing glutamate potency, we evaluated PPDA potency because the T428 residue could potentially account for the observation that NR2C has the highest affinity of the NR2s for PPDA (Feng et al., 2004) since NR2C is the only NR2 that does not have a threonine at this position. For comparison, (*R*)-CPPene, which has higher affinity for NR2B than for NR2C (Buller and Monaghan, 1997), was also tested. The 100% response of the NR1a/NR2B T428G receptor was 48 ± 5 nA.

As shown in Figure 6C, the T428G NR2B mutation increased glutamate affinity 8-fold (glutamate: wt: 2.3 ± 0.2μM; T428G: 0.26 ± 0.4μM), but had no effect on *cis*-PPDA affinity (wt: 0.31 ± 0.02μM; T428G: 0.30 ± 0.5μM) and little effect on (*R*)-CPPene affinity (wt: 0.24 ± 0.04μM; T428G: 0.14 ± 0.02μM). Thus, threonine 428 may be

contributing to the subtype-selectivity of (*S*)-glutamate for NR2C subunits but cannot account for *cis*-PPDA selectivity for NR2C or for *(R)*-CPPene selectivity for NR2B.

G713S and R712P,G713R At the edge of the binding cleft there are two additional subunit-specific residues predicted by both sets of models, G713 (NR2B numbering) and R712 (Figure 1D, 1E, 1F). NR2A and NR2B have both these residues, NR2C has a serine at the NR2B G713 position and NR2D has a proline at the R712 position (NR2B numbering) and an arginine at the G713 position. This has the effect of moving the arginine closer to the glutamate binding site in NR2D. The mutations NR2B G713S and NR2B R712P, G713R were made to mimic NR2C and NR2D, respectively. (*S*)-Glutamate and *cis*-PPDA both display higher affinity at wild type NR2C and NR2D than at NR2B. Both mutation constructs appeared to increase both (*S*)-glutamate and *cis*-PPDA affinity. The increase in *cis*-PPDA affinity at the R712P, G713R mutation was statistically significant (wt: 0.31 ± 0.02μM; R712P/G713R: 0.20 ± 0.01μM), potentially accounting for about half of the PPDA's selectivity for NR2D. The 100% response of the NR1a/NR2B G713S receptor was 44 ± 4 nA and for the NR1a/NR2B R712P,G713R receptor, 91 ± 17 nA.

Discussion

The purpose of the present study was to identify structural differences in the glutamate-binding pocket that could potentially be utilized in the design of new subtype-selective antagonists. By taking advantage of the homology between GluR2/NR1 subunits and NR2 subunits, and the recently resolved crystal structure for the GluR2 and NR1 extracellular amino acid binding domains, we generated homology models of the NR2 glutamate binding sites. The models described here predict that antagonists which are small and which only probe the immediate glutamate-binding region, are not likely to display significant NR2 subtype selectivity. Among the four NR2 subunits, 99 of the 275 amino acids (36%) in the S1/S2 domains differ between at least one of the NR2 subunits. However, our modeling suggests that only six (NR1-based model) or eight (GluR2-based model) of these variable residues are within the S1/S2 cleft (Figure 5). Furthermore, in both sets of models, five of these residues are located near the protein surface distant to bound glutamate. Thus, antagonists with large side-groups that can extend within the S1/S2 cleft towards the protein surface, may potentially interact with one of the few variant amino acid residues and thus distinguish between NR2 subunits.

The hypothesis that larger antagonists are necessary to generate varied subunit selectivity is consistent with structure-activity studies. Typically, glutamate-site NMDA receptor antagonists display slightly different affinities for NMDA receptor subunits in the order of decreasing affinity: NR2A > NR2B > NR2C > NR2D (Ikeda et al., 1992; Buller et al., 1994; Laurie and Seeburg, 1994). After surveying over 75 compounds we found only three classes of antagonists that display an atypical pattern of NR2 selectivity (Andaloro et al., 1996). These are the biphenyl piperazine compound ((2*R**,3*S**)-1-

(biphenyl-4-carbonyl)piperazine-2,3-dicarboxylic acid (PBPD), the biphenyl analogue EAB-515, and the bicyclic decahydroisoquinoline, LY233536. These compounds display an enhanced relative affinity for the NR2C and NR2D subunits and some also show higher affinities for NR2B than NR2A subunits (Buller et al., 1994; Andaloro et al., 1996; Christie et al., 2000). Thus, all antagonists that displayed an atypical selectivity pattern were large multi-ring antagonists.

Recent studies with derivatives of PBPD support the hypothesis that minor variations in antagonist structure in the distal hydrophobic region of the antagonist may vary subunit-selectivity (Feng et al., 2004). Modest changes in the biphenyl group of PBPD (such as halogenation) causes small, but significant, changes in subtype selectivity (Feng et al., 2004) and altering the ring system (e.g. biphenyl to phenanthrene) also causes significant changes in the subtype selectivity pattern. Likewise, adding a chlorine to the second phenyl ring of EAB-515 causes a preferential increase in NR1/NR2B-selectivity (Urwyler et al., 1996).

Derivatives of a new series of quinoxaline antagonists also show varied subtype-selectivity after modifications to distal moieties. The antagonist PEAQX ((R)-[(S)-1-(4-bromo-phenyl)-ethylamino]-(2,3-dioxo-1,2,3,4-tetrahydroquinoxalin-5-yl)-methyl]-phosphonic acid) has 100-fold selectivity for human NR2A over human NR2B (Auberson et al., 2002) and about 10-fold selectivity at rat NR2A vs NR2B subunits (Feng et al., 2004). This compound has a quinoxaline group in the core binding region, and a distal bromobenzene whose addition greatly increases subunit selectivity. Thus, the bromobenzene group may be extending to the edge of the S1/S2 cleft and interacting with subunit-specific residues. Furthermore, deleting the bromo group on the end of the

benzene ring significantly reduces subunit selectivity (Auberson et al., 2002).

When any of the isomers of the atypical NMDA receptor antagonist PPDA was docked to the NR2B model (GluR2-based model) we observed that the bulky and rigid phenanthrene group could fit into the S1/S2 cleft along a groove formed by two helixes (F and H; Armstrong et al., 1998). To accommodate this placement, it appears that histidine 486 may be interacting with the 2-carboxy group of *cis*-PPDA (corresponding to the β-carboxyl of aspartate or NMDA). This carboxy group of PPDA does not fit the pharmacophore models that have been generated for NMDA receptor antagonists, it is too close to the α-carboxy and amino groups (Ortwine et al., 1992; Whitten et al., 1992). Thus, H486 might be contributing to the distal acidic group binding site in the PPDA pharmacophore, but not in that of conventional antagonists. This is consistent with the observation that the NR2B H486F mutation significantly reduces *cis*-PPDA affinity, but causes a small (two-fold) increase in conventional antagonist binding affinity (CGS-19755 and PPPA; Figures 3, 4). These results are also consistent with the previous report (Laube et al., 1997) that *(R)*-AP5 and *(R)*-CPP affinities are not significantly affected by the H486F mutation. Thus, H486 appears to interact specifically with *cis*-PPDA, but not with conventional NMDA receptor antagonists that have a larger spacing between acidic groups or with *trans*-PPDA. The distal acidic group of CGS-19755, PPPA and other long chain antagonists might be interacting with K485/K488 (Tikhonova et al., 2002) and/or with T691 (Anson et al., 1998).

(S)-Glutamate affinity was also significantly reduced by the H486F mutation. These results are consistent with the modeling study of Ortwine et al., 1992 in which they concluded that agonists bind in a folded form whereas conventional antagonists have a

component of their binding site that is distal to that found in the agonist binding site. Thus, the second carboxy group of *cis*-PPDA could be binding to a site in the agonist pharmacophore (which includes H486) that is not usually occupied by antagonists.

Of the subunit-specific residues examined, NR2B A414 and T428 both may be contributing to the higher affinity displayed by (*S*)-glutamate for NR2C than for NR2B. These residues, as well as NR2B G427, did not affect antagonist binding significantly. According to the NR1-based models NR2B G427 and T428 are well outside of the ligand-binding pocket, and thus unable to interact with ligands. The effect of T428 on agonist affinity might be allosteric.

The models generated also predict that the subunit-specific residues NR2B R712 (proline in NR2D) and G713 (serine in NR2C and arginine in NR2D) may also be near enough to the S1/S2 cleft to interact with appropriate antagonists. While NR2D does not have an arginine at the position equivalent to NR2B's R712, the next residue in NR2D is an arginine which may be functionally equivalent to the NR2B R712 position. Since this residue is placed differently in the NR2D subunit, it may provide the basis for a NR2D-selective antagonist. That the 712 and 713 residues are sufficiently near the binding pocket to interact with ligands is also supported by the observation that the position corresponding to NR2B 714 in the GluR2 subunit is a residue known to interact with some AMPA receptor ligands, but not with other ligands (Armstrong et al., 1998). The NR2B G713S and NR2B R712P,G713R mutations suggest that a portion of cis-PPDA's selectivity for NR2C and NR2D could possibly be due to these subunit-specific residues.

Given the high degree of structural homology observed between the bacterial amino acid binding proteins and the S1/S2 domains of the GluR2 and NR1 subunits, it is

expected that NR2 subunits are closely related in structure to the other ionotropic glutamate receptors. Consequently, it is likely that the GluR1-7 and KA1/2 subunits are also conserved in the general shape of S1/S2 glutamate binding cleft. Thus, within these families, development of larger antagonists that probe the S1/S2 cleft may yield high affinity antagonists. For the glycine binding site of NR1, the bulky compound L-701,324 (7-chloro-4-hydroxy-3-(3-phenoxy)phenyl-2(H)-quinolinone) (Kulagowski et al., 1994) may represent such an antagonist. At the same time, it might be expected that large antagonists with side-groups which reach the subunit-specific regions of the S1/S2 cleft could have modified subtype-selectivity. One potential example of such a subtype-selective ligand is LY339434 ((2*S*,4*R*,6*E*)-2-amino-4-carboxy-7-(2-naphthyl)hept-6-enoate). This compound is a kainate receptor agonist derivative of (2*S*,4*R*)-4-methylglutamate (Small et al., 1998). By replacing the methyl group with a bulky naphthalene ring on a propenyl linker at the 4-position of glutamate, GluR5 affinity is reduced 5-fold whereas GluR6 affinity is reduced over 1000-fold. Thus, addition of a distal hydrophobic ring system markedly enhances KA receptor subunit selectivity.

Overall, these studies suggest that there are relatively few amino acid residues in the NR2 subunits that may be capable of conferring subunit-specific antagonist binding. Importantly, however, there does appear to be at least one significantly different residue that is unique to each of the four NR2 subunits that may be near enough to interact with an appropriately designed antagonist molecule.

Acknowledgments:

The authors wish to thank Dr. Mike Sturgess for providing a copy of the NR2 model based upon the LAOBP structure. We also gratefully acknowledge Drs. Shigetada Nakanishi, David Lynch, Dolan Pritchett, and Peter Seeburg for providing cDNA constructs, and Dr. Paul Ornstein and Dr. Richard Lovell for providing antagonist compounds.

References:

Andaloro VJ, Jane DJ, Tse HW, Watkins JC and Monaghan DT (1996) Pharmacology of NMDA receptor subtypes. *Society for Neuroscience Abstracts* **604**.

Anson LC, Chen PE, Wyllie DJA, Colquhoun D and Schoepfer R (1998) Identification of amino acid residues of the NR2A subunit that control glutamate potency in recombinant NR1/NR2A NMDA receptors. *J Neurosci* **18**:581-589.

Armstrong N and Gouaux E (2000) Mechanisms for activation and antagonism of an AMPA-sensitive glutamate receptor: crystal structures of the GluR2 ligand binding core. *Neuron* **28**:165-181.

Armstrong N, Sun Y, Chen GQ and Gouaux E (1998) Structure of a glutamate-receptor ligand-binding core in complex with kainate. *Nature* **395**:913-917.

Auberson YP, Allgeier H, Bischoff S, Lingenhoehl K, Moretti R and Schmutz M (2002) 5-Phosphonomethylquinoxalinediones as competitive NMDA receptor antagonists with a preference for the human 1A/2A, rather than 1A/2B receptor composition. *Bioorg Med Chem Lett* **12**:1099-1102.

Bear MF, Kleinschmidt A, Gu QA and Singer W (1990) Disruption of experience-dependent synaptic modifications in striate cortex by infusion of an NMDA receptor antagonist. *J Neurosci* **10**:909-925.

Beaton JA, Stemsrud K and Monaghan DT (1992) Identification of a novel N-methyl-D-aspartate receptor population in the rat medial thalamus. *J Neurochem* **59**:754-757.

Bigge CF (1993) Structural requirements for the development of potent N-methyl-D-aspartic acid (NMDA) receptor antagonists. *Biochem Pharmacol* **45**:1547-1561.

Buller AL, Larson HC, Schneider BE, Beaton JA, Morrisett RA and Monaghan DT (1994) The molecular basis of NMDA receptor subtypes: native receptor diversity is predicted by subunit composition. *J Neurosci* **14**:5471-5484.

Buller AL and Monaghan DT (1997) Pharmacological heterogeneity of NMDA receptors: characterization of NR1a/NR2D heteromers expressed in Xenopus oocytes. *Eur J Pharmacol* **320**:87-94.

Cheung NS, D OC, Ryan MC, Dutton R, Wong MG and Beart PM (1996) Structure-activity relationships of competitive NMDA receptor antagonists. *Eur J Pharmacol* **313**:159-162.

Choi DW (1992) Excitotoxic cell death. *J Neurobiol* **23**:1261-1276.

Christie JM, Jane DE and Monaghan DT (2000) Native N-Methyl-D-aspartate Receptors Containing NR2A and NR2B Subunits Have Pharmacologically Distinct Competitive Antagonist Binding Sites. *J Pharmacol Exp Ther* **292**:1169-1174.

Collingridge GL and Bliss TV (1995) Memories of NMDA receptors and LTP. *Trends Neurosci* **18**:54-56.

Feng B, Tse HW, Skifter DA, Morley R, Jane DE and Monaghan DT (2004) Structure-activity analysis of a novel NR2C/NR2D-preferring NMDA receptor antagonist: 1-(phenanthrene-2-carbonyl) piperazine-2,3-dicarboxylic acid. *Br J Pharmacol* **141**:508-516.

Furukawa H and Gouaux E (2003) Mechanisms of activation, inhibition and specificity: crystal structures of the NMDA receptor NR1 ligand-binding core. *Embo J* **22**:2873-2885.

Ikeda K, Nagasawa M, Mori H, Araki K, Sakimura K, Watanabe M, Inoue Y and Mishina M (1992) Cloning and expression of the epsilon 4 subunit of the NMDA receptor channel. *FEBS Lett* **313**:34-38.

Ishii T, Moriyoshi K, Sugihara H, Sakurada K, Kadotani H, Yokoi M, Akazawa C, Shigemoto R, Mizuno N, Masu M and al. e (1993) Molecular characterization of the family of the N-methyl-D-aspartate receptor subunits. *J Biol Chem* **268**:2836-2843.

Kulagowski JJ, Baker R, Curtis NR, Leeson PD, Mawer IM, Moseley AM, Ridgill MP, Rowley M, Stansfield I, Foster AC and et al. (1994) 3'-(Arylmethyl)- and 3'-(aryloxy)-3-phenyl-4-hydroxyquinolin-2(1H)- ones: orally active antagonists of the glycine site on the NMDA receptor. *J Med Chem* **37**:1402-1405.

Laube B, Hirai H, Sturgess M, Betz H and Kuhse J (1997) Molecular determinants of agonist discrimination by NMDA receptor subunits: analysis of the glutamate binding site on the NR2B subunit. *Neuron* **18**:493-503.

Laube B, Kuhse J and Betz H (1998) Evidence for a tetrameric structure of recombinant NMDA receptors. *J Neurosci* **18**:2954-2961.

Laurie DJ and Seeburg PH (1994) Ligand affinities at recombinant N-methyl-D-aspartate receptors depend on subunit composition. *Eur J Pharmacol* **268**:335-345.

Monaghan DT, Bridges RJ and Cotman CW (1989) The excitatory amino acid receptors: their classes, pharmacology, and distinct properties in the function of the central nervous system. *Annu Rev Pharmacol Toxicol* **29**:365-402.

Monaghan DT and Larson H (1997) NR1 and NR2 subunit contributions to N-methyl-D-aspartate receptor channel blocker pharmacology. *J Pharmacol Exp Ther* **280**:614-620.

Monaghan DT, Olverman HJ, Nguyen L, Watkins JC and Cotman CW (1988) Two classes of N-methyl-D-aspartate recognition sites: differential distribution and differential regulation by glycine. *Proc Natl Acad Sci U S A* **85**:9836-9840.

Monyer H, Burnashev N, Laurie DJ, Sakmann B and Seeburg PH (1994) Developmental and regional expression in the rat brain and functional properties of four NMDA receptors. *Neuron* **12**:529-540.

Monyer H, Sprengel R, Schoepfer R, Herb A, Higuchi M, Lomeli H, Burnashev N, Sakmann B and Seeburg PH (1992) Heteromeric NMDA receptors: molecular and functional distinction of subtypes. *Science* **256**:1217-1221.

Nakanishi N, Shneider NA and Axel R (1990) A family of glutamate receptor genes: evidence for the formation of heteromultimeric receptors with distinct channel properties. *Neuron* **5**:569-581.

O'Hara PJ, Sheppard PO, Thogersen H, Venezia D, Haldeman BA, McGrane V, Houamed KM, Thomsen C, Gilbert TL and Mulvihill ER (1993) The ligand-binding domain in metabotropic glutamate receptors is related to bacterial periplasmic binding proteins. *Neuron* **11**:41-52.

Oh BH, Pandit J, Kang CH, Nikaido K, Gokcen S, Ames GF and Kim SH (1993) Three-dimensional structures of the periplasmic lysine/arginine/ornithine-binding protein with and without a ligand. *J Biol Chem* **268**:11348-11355.

Ortwine DF, Malone TC, Bigge CF, Drummond JT, Humblet C, Johnson G and Pinter GW (1992) Generation of N-methyl-D-aspartate agonist and competitive antagonist pharmacophore models. Design and synthesis of phosphonoalkyl-substituted tetrahydroisoquinolines as novel antagonists. *J Med Chem* **35**:1345-1370.

Small B, Thomas J, Kemp M, Hoo K, Ballyk B, Deverill M, Ogden AM, Rubio A, Pedregal C and Bleakman D (1998) LY339434, a GluR5 kainate receptor agonist. *Neuropharmacology* **37**:1261-1267.

Sucher NJ, Akbarian S, Chi CL, Leclerc CL, Awobuluyi M, Deitcher DL, Wu MK, Yuan JP, Jones EG and Lipton SA (1995) Developmental and regional expression pattern of a novel NMDA receptor-like subunit (NMDAR-L) in the rodent brain. *J Neurosci* **15**:6509-6520.

Sugihara H, Moriyoshi K, Ishii T, Masu M and Nakanishi S (1992) Structures and properties of seven isoforms of the NMDA receptor generated by alternative splicing. *Biochem Biophys Res Commun* **185**:826-832.

Tikhonova IG, Baskin, II, Palyulin VA and Zefirov NS (2002) Computer simulation of the three-dimensional structure of the glutamate site of the NR2B subunit of the NMDA receptor. *Dokl Biochem Biophys* **382**:38-41.

Urwyler S, Campbell E, Fricker G, Jenner P, Lemaire M, McAllister KH, Neijt HC, Park CK, Perkins M, Rudin M, Sauter A, Smith L, Wiederhold KH and Muller W (1996) Biphenyl-derivatives of 2-amino-7-phosphono-heptanoic acid, a novel class of potent competitive N-methyl-D-aspartate receptor antagonists--II. Pharmacological characterization in vivo. *Neuropharmacology* **35**:655-669.

Watanabe M, Inoue Y, Sakimura K and Mishina M (1993) Distinct spatio-temporal distributions of the NMDA receptor channel subunit mRNAs in the brain. *Ann N Y Acad Sci* **707**:463-466.

Watkins JC and Evans RH (1981) Excitatory amino acid transmitters. *Annu Rev Pharmacol Toxicol* **21**:165-204.

Watkins JC, Krogsgaard Larsen P and Honore T (1990) Structure-activity relationships in the development of excitatory amino acid receptor agonists and competitive antagonists. *Trends Pharmacol Sci* **11**:25-33.

Whitten JP, Harrison BL, Weintraub HJ and McDonald IA (1992) Modeling of competitive phosphono amino acid NMDA receptor antagonists. *J Med Chem* **35**:1509-1514.

Footnotes:

This work was supported by NIH grant MH60252. Reprint requests should be sent to Dr. Dan Monaghan, 985800 Nebraska Medical Center, Omaha, NE 68198-5800.

[1] These two authors contributed equally to this manuscript.

Legends for Figures:

Figure 1

NR2 S1/S2 molecular models. A. Tube representation of homology models of the S1 and S2 domains of NR2B (red) and NR2C (blue) superimposed upon the resolved crystal structure of GluR2's S1/S2 domains (green). In the center, kainate (stick representation) is shown in GluR2 as determined by crystalography. The extra loop of the NR2s that is absent in GluR2 is found immediately to the right of kainate (note the absence of the green chain). B. The ligand-binding cleft of NR2B is shown docked to *cis*-PPDA. The phenanthrene ring of *cis*-PPDA lies in the S1/S2 cleft in a groove formed from the base of two alpha helicies. Histidine 468 is above the 2-position carboxylate group of PPDA. In the GluR2 subunit, the corresponding carboxy group (ω) in kainic acid interacts with residues homologous to S690 and T691. Other critical ligand binding residues are also shown; T514 and D732 whose GluR2 equivalents bind the α amino group of *(S)*-glutamate in GluR2 and R519 corresponding to the arginine in GluR2 that binds the α-carboxy group of *(S)*-glutamate. C. Amino acid residues of the NR2s that are not identical for all four of the NR2s are shown as magenta amino acid residues with side chains on the GluR2-based NR2B homology model (blue tube structure). Note that variable amino acid residues are predominately found on the protein surface and not in the ligand-binding pocket. The yellow tube portion represents a disulfide bridge predicted from the GluR2 crystal structure. D. In the GluR2-based NR2B homology model (blue tube) the positions of the conserved amino acids lining the ligand-binding pocket are shown in green while the variable amino acids of the pocket are shown with side-chains in magenta. The conserved critical ligand binding amino acids are shown with side chains in red (oxygen), white, and blue (nitrogens). E. Side-view of the figure in D

showing the subunit-specific residues at the front of the binding pocket. F. The human NR1-based NR2B S1/S2 domain homology model in a representation and orientation similar to that in D.

Figure 2

Structures of NMDA receptor antagonists used, or discussed, in this study.

Figure 3

Differential interactions of NR2B histidine 486 with different glutamate-binding site ligands. Dose-response analysis of the activation and inhibition of NR1a/NR2B and NR1a/NR2B H486F shows that the EC50s for (*S*)-glutamate and *cis*-PPDA were increased by the mutation (i.e. lower affinity), while the EC50s for *trans*-PPDA and the longer chain antagonists CGS-19755 and PPPA were reduced by the mutation. Mean values are shown ± S.E.M.. All experiments were performed at least 4 times.

Figure 4

The differential effect of the NR2B H486F mutation on the affinities for (*S*)-glutamate, *cis*- and *trans*-PPDA, CGS-19755, and PPPA are shown. The affinity values shown are normalized by dividing the measured affinity (Kd for (*S*)-glutamate , Ki for the antagonists) by the corresponding affinity at NR2B wild type (WT) receptors. The Ki values were corrected for mutation-induced changes in (*S*)-glutamate affinity. Asterisks indicate a statistically-significant difference, * $p<0.05$, ** $p < 0.01$, *** $p < 0.001$ between WT and mutant receptors.

Figure 5

Sequence alignment for the S1 and S2 domains of NR2 subunits. Amino acids lining the ligand-binding cleft in the GluR2-based homology models are shown in boxes. The amino acid residues that are non-identical among the four NR2 subunits and lining the ligand-binding cleft are shown in bold. The NR1-based homology models predicted the same cleft residues except for the second set of amino acids (ETC for NR2A) that were predicted to be outside of the ligand-binding cleft. The location of NR2BH486 is shown with an asterisk. The single ligand-binding pocket amino acid differing between rat and human sequences (NR2A R711) is shown with an arrow.

Figure 6

The effect of mutating NR2B subunit-specific amino acid residues on agonist and antagonist affinities. Agonist (Kd) and antagonist (Ki) affinities at mutant and wild type (WT) receptors were normalized by dividing by the corresponding affinity at WT NR1a-NR2B and expressed as mean ± S.E.M.. The measured (*S*)-glutamate affinities were used to determine antagonist Ki values. All experiments were performed at least 4 times. A. The NR2B A414R mutation replaces in NR2B the equivalent residues from NR2C and NR2D ("B-C,D"). This mutation was tested for (*S*)-glutamate, NMDA, and LY233536 affinity and compared to the affinities of these compounds for receptors containing NR2B, NR2C, and NR2D subunits. B. The NR2B G427E mutation places the residue found in NR2A into the equivalent position of NR2B. This mutation did not affect agonist affinity or the NR2B-selective agonist LY233536. C. The NR2B T428G mutant

has T428 replaced by the equivalent residue (G) from the NR2C subunit and its affinities for (*S*)-glutamate, *cis*-PPDA, and D-CPPene were compared to NR2B and NR2C-containing NMDA receptors. D. Residues 712 and 713 of NR2B were modified to mimic the equivalent residues found in NR2C (NR2B G713S) and in NR2D (NR2B R712P,G713R). These were tested with (*S*)-glutamate and *cis*-PPDA which display higher affinities for NR2C and NR2D than for NR2B. Asterisks indicate a statistically-significant difference, between NR2B and mutant, * $p<0.05$, ** $p < 0.01$, *** $p < 0.001$. For comparison, corresponding values for NR2A, NR2C and NR2D (Buller and Monaghan, 1997) are shown when appropriate.

JPET Fast Forward. Published on March 2, 2005 as DOI: 10.1124/jpet.104.082990
This article has not been copyedited and formatted. The final version may differ from this version.

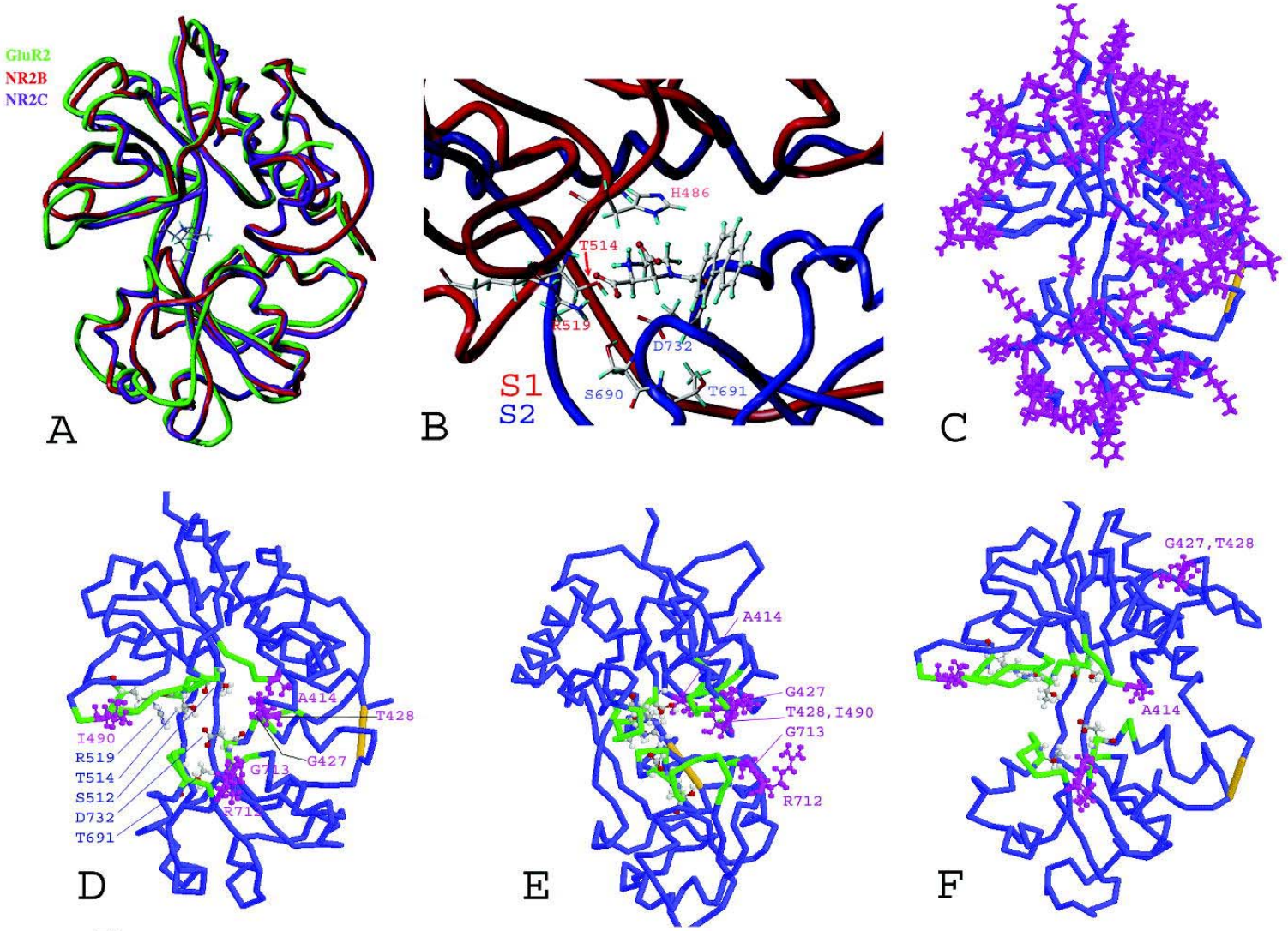

Fig. 1

JPET Fast Forward. Published on March 2, 2005 as DOI: 10.1124/jpet.104.082990

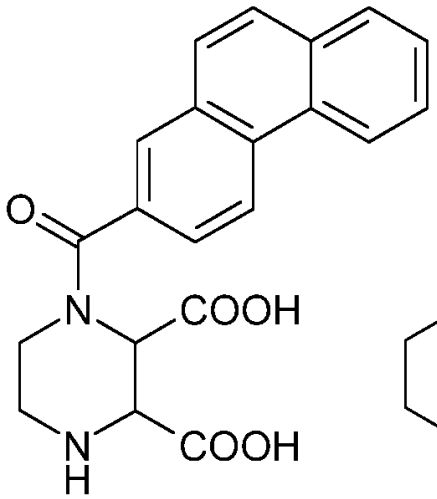

PPDA

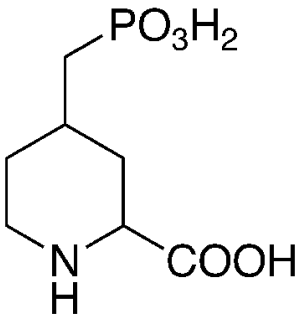

CGS19755

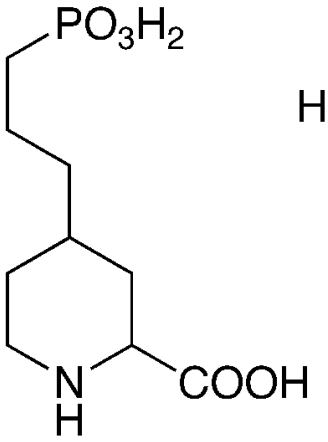

PPPA

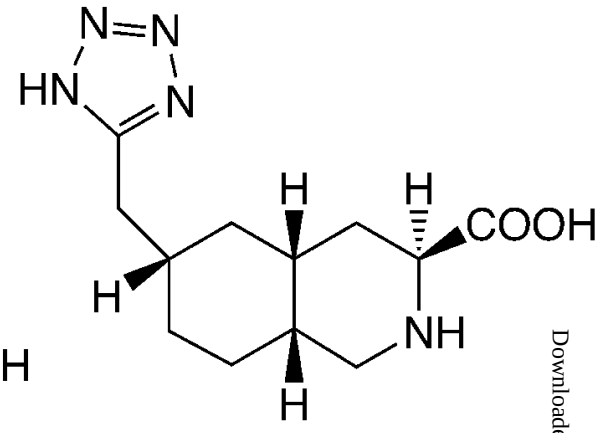

LY233536

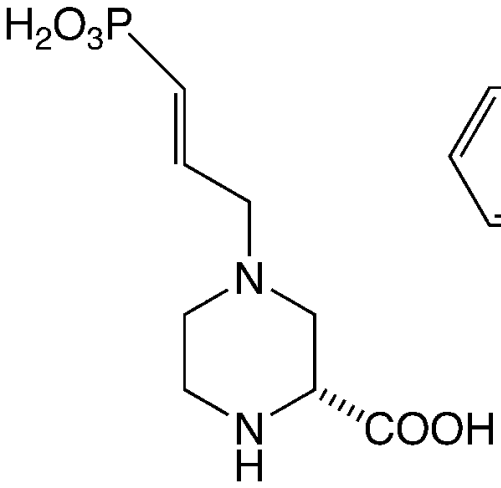

(R)-CPPene

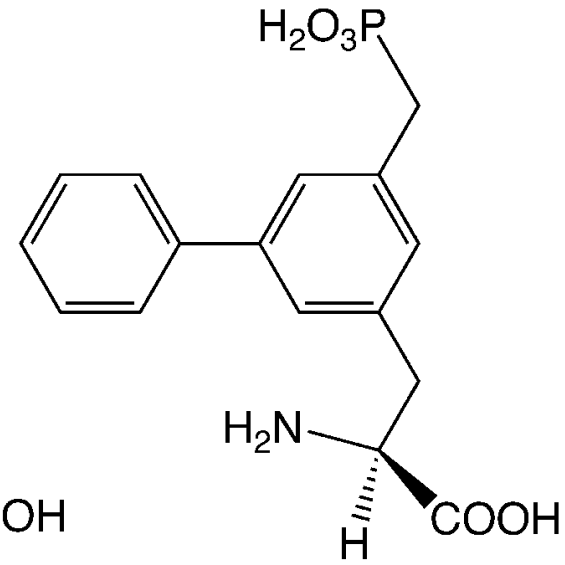

EAB515

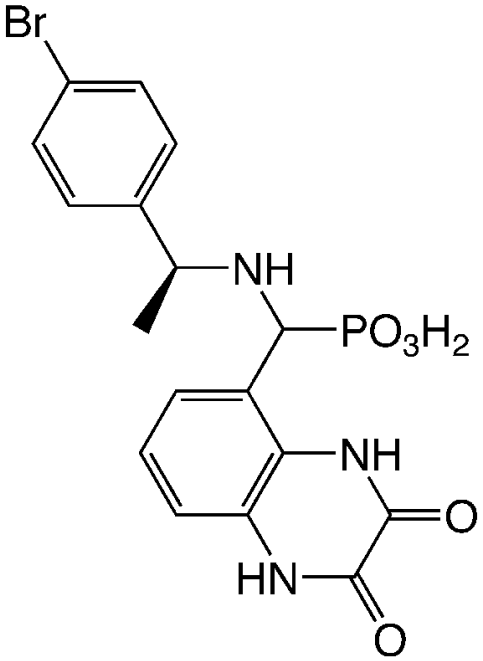

PEAQX

Fig. 2

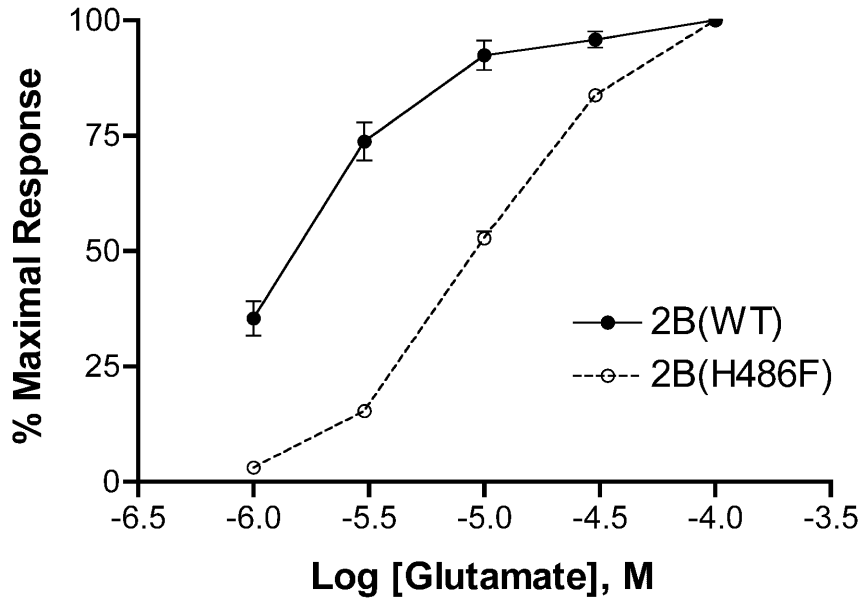

A

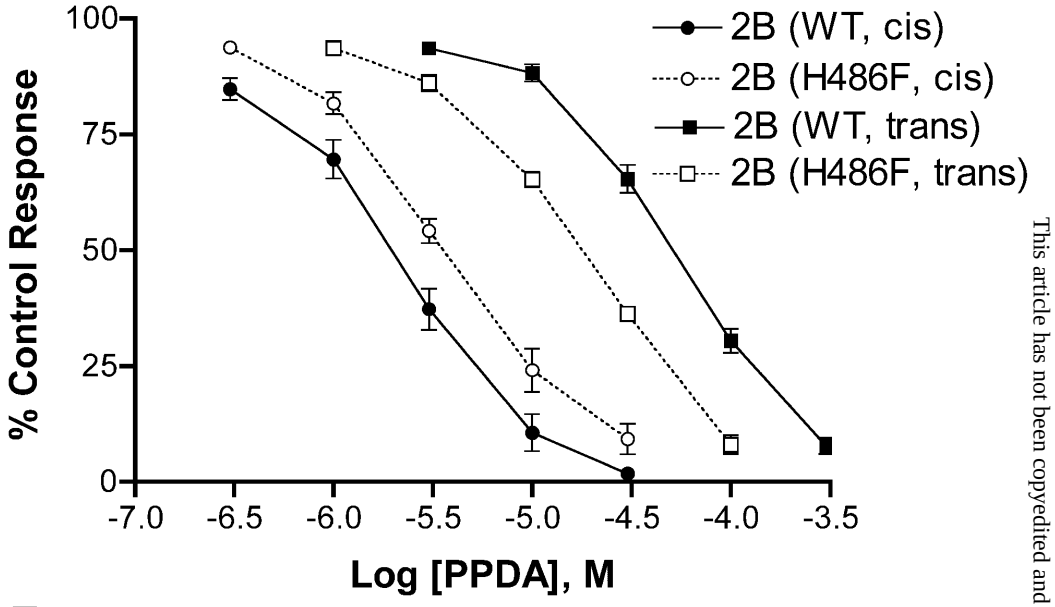

B

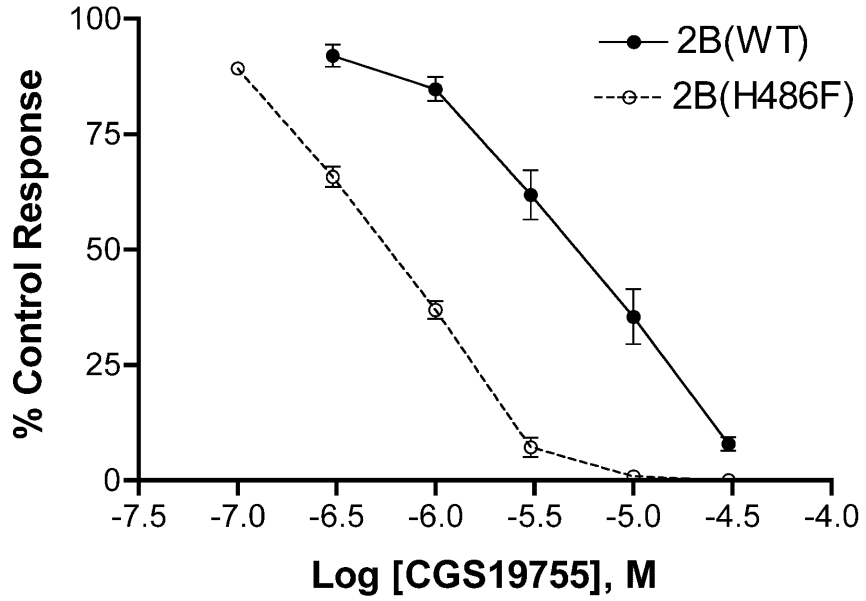

C

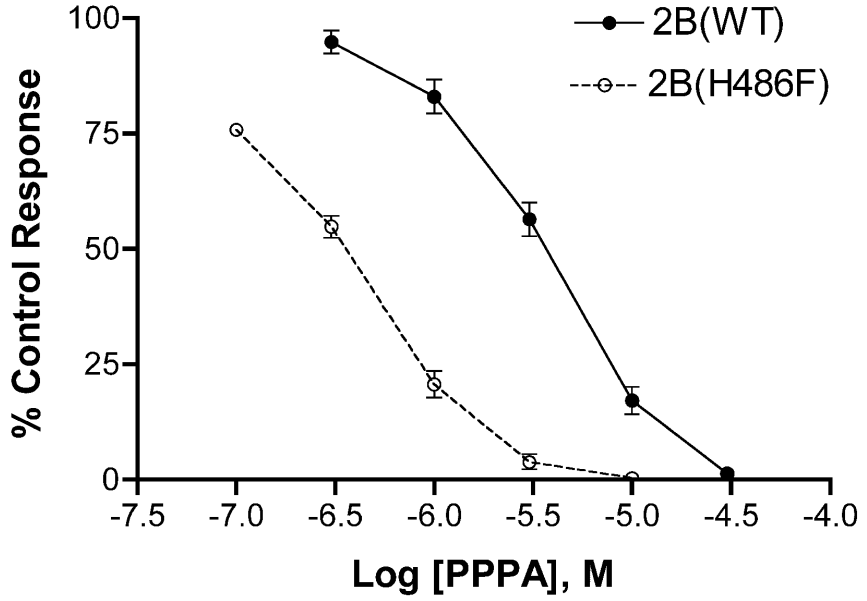

D

Fig. 3

JPET Fast Forward. Published on March 2, 2005 as DOI: 10.1124/jpet.104.082990
This article has not been copyedited and formatted. The final version may differ from this version.

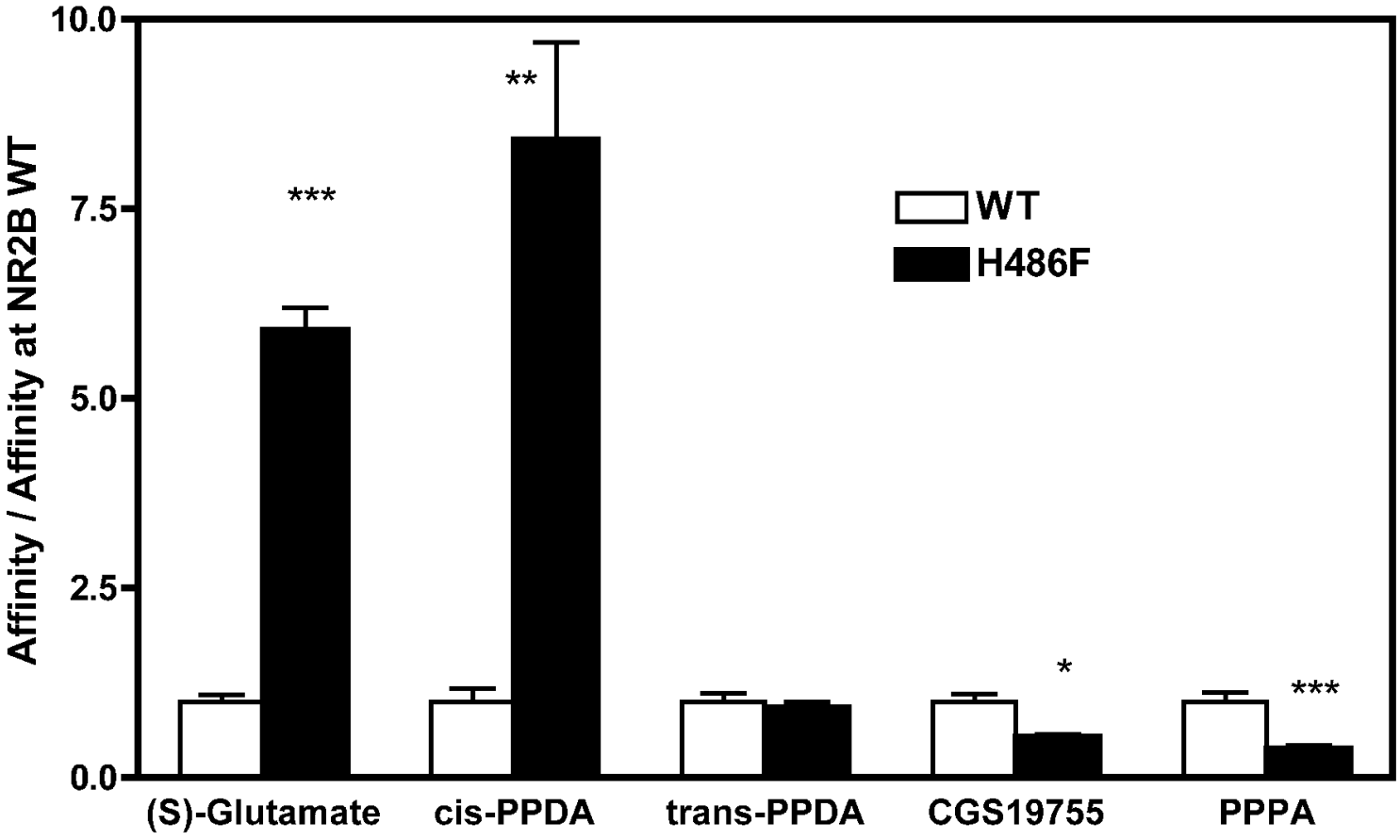

Fig. 4

JPET Fast Forward. Published on March 2, 2005 as DOI: 10.1124/jpet.104.082990
This article has not been copyedited and formatted. The final version may differ from this version.

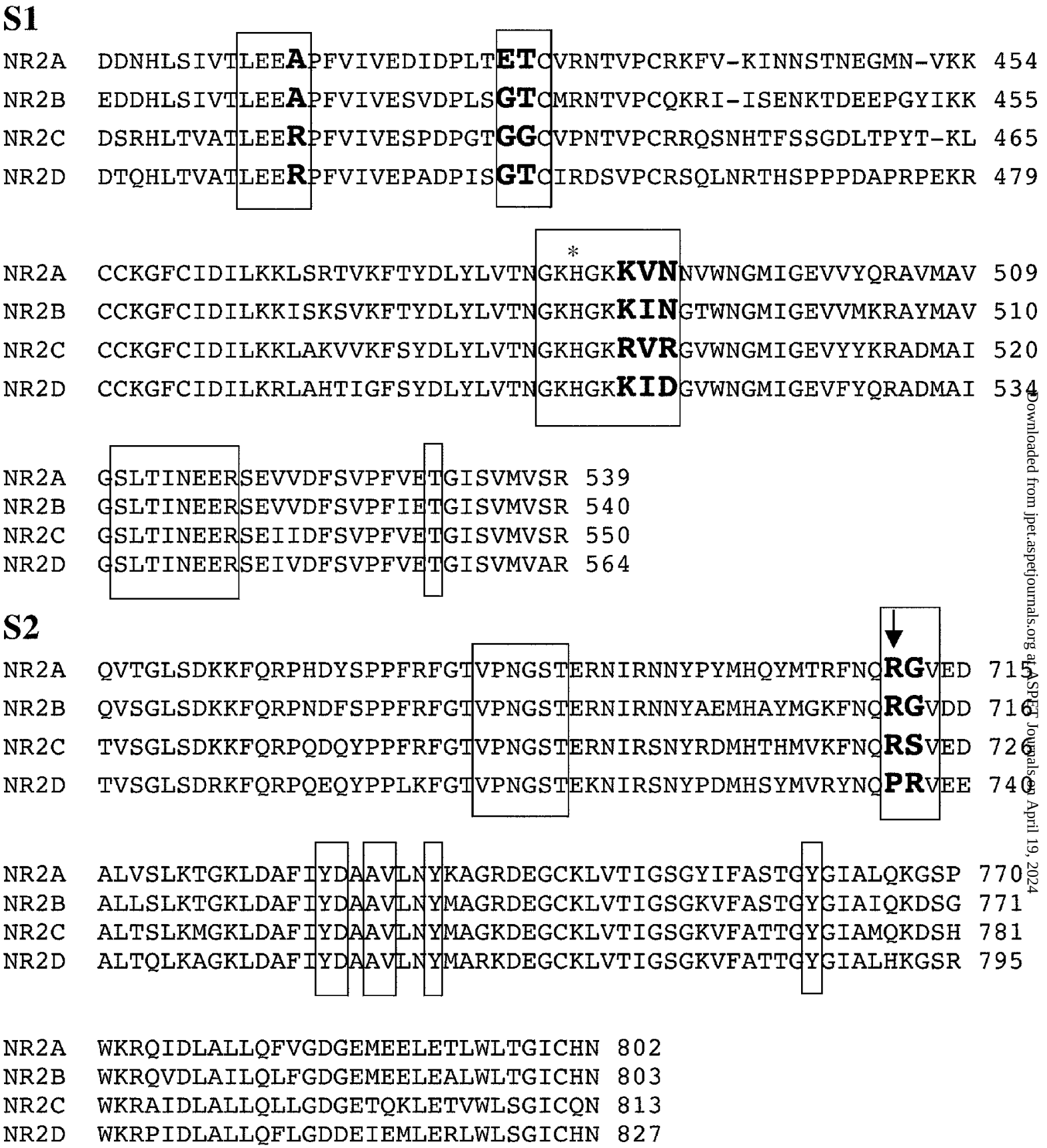

Fig. 5

JPET Fast Forward. Published on March 2, 2005 as DOI: 10.1124/jpet.104.082990
This article has not been copyedited and formatted. The final version may differ from this version.

***

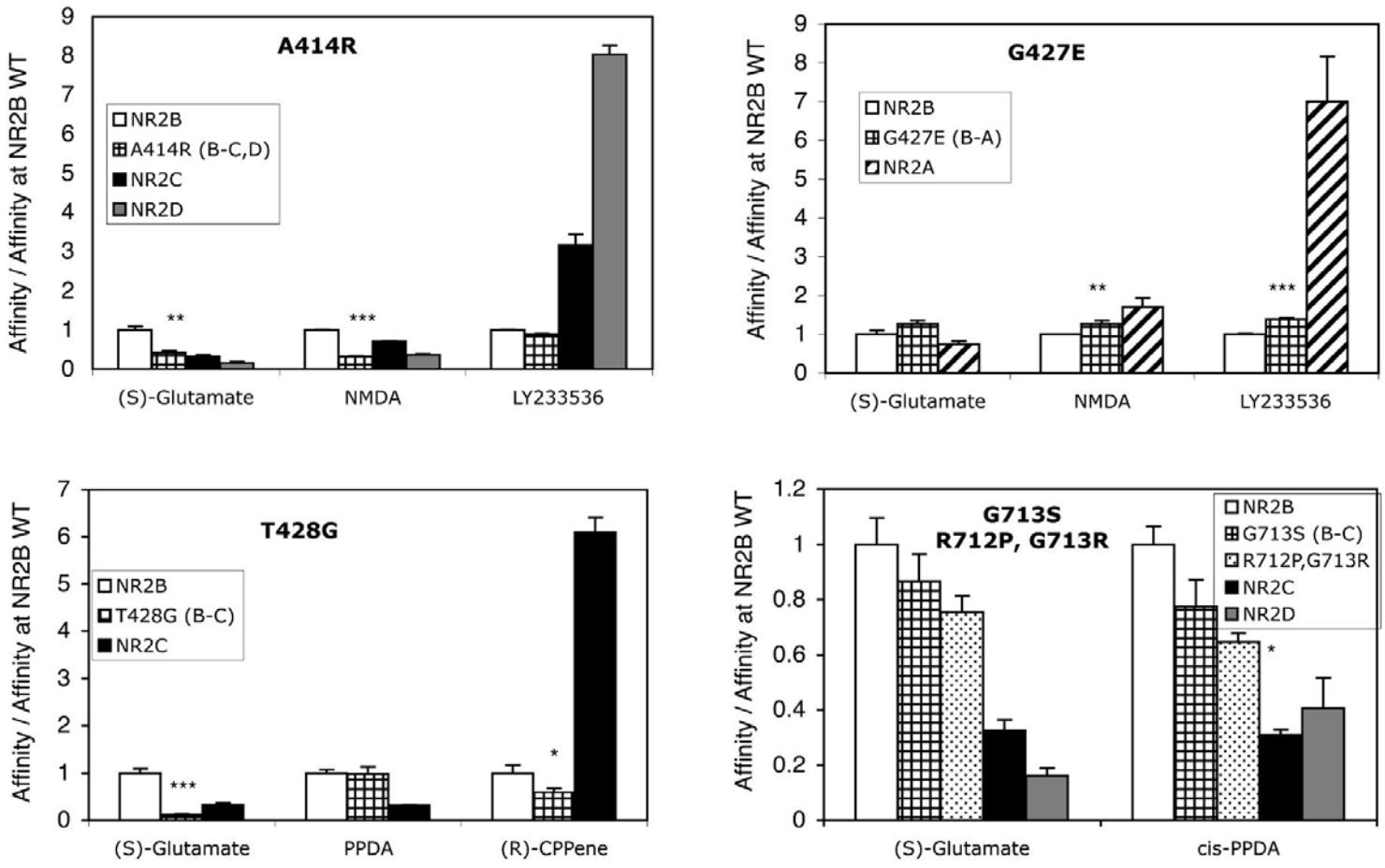

Fig. 6